Hindawi Publishing Corporation
International Journal of Electrochemistry
Volume 2014, Article ID 768912, 9 pages
http://dx.doi.org/10.1155/2014/768912

Research Article

Synthesis and Electrochemical Performance of $LiMnPO_4$ by Hydrothermal Method

Daichi Fujimoto,[1,2] Yu Lei,[1] Zheng-Hong Huang,[1] Feiyu Kang,[1] and Junichi Kawamura[2]

[1] *Key Laboratory of Advanced Materials (MOE), School of Materials Science and Engineering, Tsinghua University, Beijing 100084, China*
[2] *Institute of Multidisciplinary Research for Advanced Materials, Tohoku University, Sendai 980-8577, Japan*

Correspondence should be addressed to Feiyu Kang; fykang@tsinghua.edu.cn

Received 14 March 2014; Accepted 4 June 2014; Published 8 July 2014

Academic Editor: Shengshui Hu

$LiMnPO_4$ with olivinestructure which is the promising candidate for high voltage cathode material was synthesized by hydrothermal method. In order to synthesize high purity and well-defined $LiMnPO_4$, several precursors for Li, Mn, and P sources and hydrothermal reaction parameters including temperature and $[H_2O]/[Mn]$ value are optimized. By analyzing the structure, Mn valence, morphology, and chemical ratio via XRD, XPS, Raman, SEM, and ICP $LiMnPO_4$ synthesized from manganese acetate tetrahydrate have single phase of $LiMnPO_4$ without impurity and showed charge and discharge reaction caused by Mn^{2+}/Mn^{3+} redox. Specific capacity of synthesized $LiMnPO_4$ grew up during cycling. Moreover, when hydrothermal temperature was set at 150°C and $[H_2O]/[Mn]$ value was set at 15, discharge capacity as high as 70 mAh/g was obtained at 1/20 *C* rate.

1. Introduction

Lithium-ion batteries are used widely as mobile devices like cellphone and notebook. Recently, researchers are actively devoted into the lithium-ion battery research for high energy conversion system, such as electric vehicle. Most of present lithium-ion batteries have used $LiCoO_2$ as cathode which was discovered in 1980 [1]. However, $LiCoO_2$ which includes rare-metal Co has irreversible structure shift at discharging over 0.6 Li from $LiCoO_2$ that cause discharge capacity limited to 120~130 mAh/g instead of theoretical capacity of 270 mAh/g [2]. Several alternative materials are proposed as cathode materials. In 1997, Padhi et al. reported that phospho-olivine can work as promising cathode materials for lithium-ion battery [3, 4]. Among phospho-olivine $LiFePO_4$, $LiMnPO_4$, $LiCoPO_4$, and $LiNiPO_4$ are considered to be possible candidates for lithium-ion battery. Compared to $LiFePO_4$ and $LiCoPO_4$, $LiMnPO_4$ is a cathode material with high redox potential which can be used with presently available liquid electrolyte so that $LiMnPO_4$ exceeds the energy density of $LiFePO_4$ which is the most investigated electrode among $LiMPO_4$ family [5]. The characteristic of this olivine structure is an inductive effect which appears due to a strong covalent bond of PO_4^- to rise up redox potential [3]. However, the strong covalent bond causes poor conductivity, decelerating the charge and discharge processes. So far, several approaches have been used to solve this problem, such as controlling the particle size, morphology, and carbon coating [6]. Solid state reaction is generally used to prepare $LiMnPO_4$ [7, 8]. Besides this, other approaches such as sol-gel method [9, 10], precipitation [11–13], hydrothermal [10, 14–19], solvothermal method [14, 20–22], spray pyrolysis [23], and polyol process [24, 25] are also used. The hydrothermal method is a simple synthesis method in which precursors are put into autoclave with water and seal and heat at around 200°C. The advantages of hydrothermal method are the capability of synthesizing at low temperature, obtaining high crystallinity, high purity material, and controlling particle size and morphology. Therefore, in this work, we further optimized synthesis parameters of hydrothermal method for $LiMnPO_4$ synthesis and investigated their electrochemical performance.

2. Experimental

2.1. Preparation of $LiMnPO_4$. The hydrothermal reaction of $LiMnPO_4$ was carried out under various conditions at 150°C

Table 1: The list of precursors and conditions for sample preparation.

	Sample	Precursors			Temperature	$[H_2O]/[Mn]$ value
Various precursors	Sample A	LiAc	MnAc	$NH_4H_2PO_4$	190°C	30
	Sample B	LiOH	MnAc	$NH_4H_2PO_4$	190°C	30
	Sample C	LiAc	$MnSO_4$	$NH_4H_2PO_4$	190°C	30
	Sample D	LiOH	$MnSO_4$	$NH_4H_2PO_4$	190°C	30
Various conditions	Sample B	LiOH	MnAc	$NH_4H_2PO_4$	190°C	30
	Sample E	LiOH	MnAc	$NH_4H_2PO_4$	190°C	15
	Sample F	LiOH	MnAc	$NH_4H_2PO_4$	150°C	30
	Sample G	LiOH	MnAc	$NH_4H_2PO_4$	150°C	15

or 190°C for 12 hours after Li, Mn, and P source with stoichiometric ratio were dispersed uniformly with distilled water. Lithium acetate dihydrate (denoted as LiAc) and lithium hydroxide monohydrate (LiOH) were the candidates for Li source, manganese acetate tetrahydrate (MnAc) and manganese sulfate monohydrate ($MnSO_4$) worked as Mn source, and ammonium dihydrogen phosphate ($NH_4H_2PO_4$) was P source. The amount of water was set as $[H_2O]/[Mn]$ = 15 or 30. Herein, samples are denoted as A, B, C, D, E, F, and G depending on synthesis conditions. The samples preparation conditions are listed in Table 1. These precursors were put into autoclave with quantitative distilled water and stirred by magnetic stirrer. This solution was put into oven with 2.5°C/min heating rate. After keeping 12 hours, the autoclave was naturally cooled down to room temperature. Finally, the powder was washed with distilled water and ethanol several times by centrifugation and dried out at 100°C for about 12 hours.

2.2. Characterization. The crystalline phases were identified by X-ray diffraction (XRD, D/max-2500, Rigaku) with Cu-Kα radiation. The oxidation state of manganese was confirmed by the X-ray photoelectron spectroscopy (XPS, ESCALAB 250Xi, Thermo Scientific). The composition analysis of Li, Mn, and P was carried out using inductively coupled plasma (ICP-OES, VISTA-MPX) by dissolving $LiMnPO_4$ powder into aqua regia. The morphology and particle size were observed by scanning electron microscope (SEM, LEO-1530). The existence of impurity was confirmed by Raman spectroscopy (Lab RAMHR800, HORIBA Jobin Yvon Ltd., USA) with 488 nm wavelength laser.

2.3. Electrochemical Measurement. The synthesized $LiMnPO_4$ by hydrothermal reaction was mixed and smashed with carbon black (weight was set to 1/8 of $LiMnPO_4$) by wet ball milling with ethanol for 3 hours. After evaporating ethanol, this mixture was followed by dry ball milling for 3 hours to obtain well-mixed $LiMnPO_4$/C compound.

The electrochemical measurement was performed by constant current cyclic voltammetry using 2032 coin-cell battery for evaluation of specific capacity. $LiMnPO_4$/C compound was mixed with PVDF (polyvinyliden fluoride: Shenzhen Kejing Star Technology Company) and carbon black (Shenzhen Kejing Star Technology Company) and then dispersed in NMP (N-methylpyrrolidone: Shenzhen Kejing Star Technology Company). Then, the slurry was stirred by magnet stirrer for several hours. The final weight ratio of $LiMnPO_4$: carbon black : PDVF was set as 70 : 20 : 10. The solution was then pasted on aluminum foil followed by drying at 80°C for 2 hours and then 120°C in vacuum for 12 hours. After vacuum for half day, this foil was naturally cooled down to room temperature in vacuum and cut to disc with 10 mm of diameter. Lithium disc was used as counter electrode, and EC:DMC (1 mol/L $LiPF_6$) was used as electrolyte and a celgard 2400 was used as separator. 2032 coin-cell battery (CR-2032) was assembled in glove box filled by Ar gas. After 1 day, galvanostatic charge and discharge were carried out at 1/20 C rate for 50 cycles using LAND battery test (Wuhan Jinnuo Electronics Co., Ltd.).

Table 2: Binding energy of $Mn2p_{3/2}$ for $LiMnPO_4$ using various precursors.

Sample	$Mn2p_{3/2}$ [eV]
Sample A	641.58
Sample B	641.57
Sample C	642.04
Sample D	641.99

3. Results and Discussion

3.1. Effect of Different Precursors on Hydrothermal Synthesis of $LiMnPO_4$. XRD pattern of all the samples is shown in Figure 1. Samples synthesized from MnAc as Mn source (samples A and B) have $LiMnPO_4$ crystal structure. All peaks come from $LiMnPO_4$ diffraction pattern, and no impurity was observed. However, diffraction pattern corresponding to $Mn_2P_2O_7$ rather than $LiMnPO_4$ was observed in the XRD patterns of samples synthesized from $MnSO_4$ (samples C and D).

XPS measurement was performed to evaluate Mn valence in $LiMnPO_4$. The narrow scan XPS spectra in Figure 2(b) suggest that the binding energy of $Mn2p_{3/2}$ is around 641.6 eV in samples A and B synthesized from MnAc. On the other hand, the binding energy of $Mn2p_{3/2}$ is around 642.0 eV in samples C and D synthesized from $MnSO_4$ (Table 2). Since the Mn^{2+} has lower oxidation state than Mn^{3+}, therefore

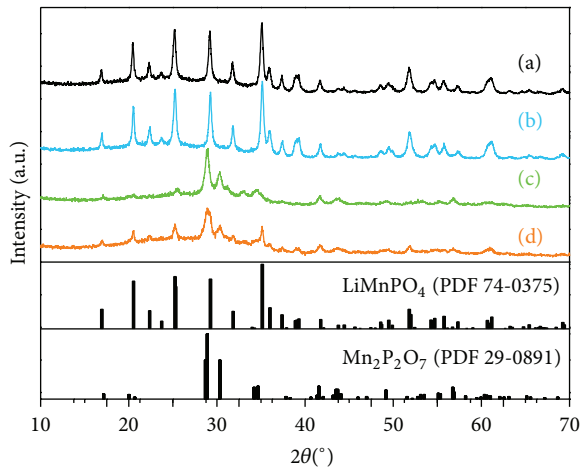

Figure 1: XRD pattern for $LiMnPO_4$ using various precursors: (a) sample A, (b) sample B, (c) sample C, and (d) sample D.

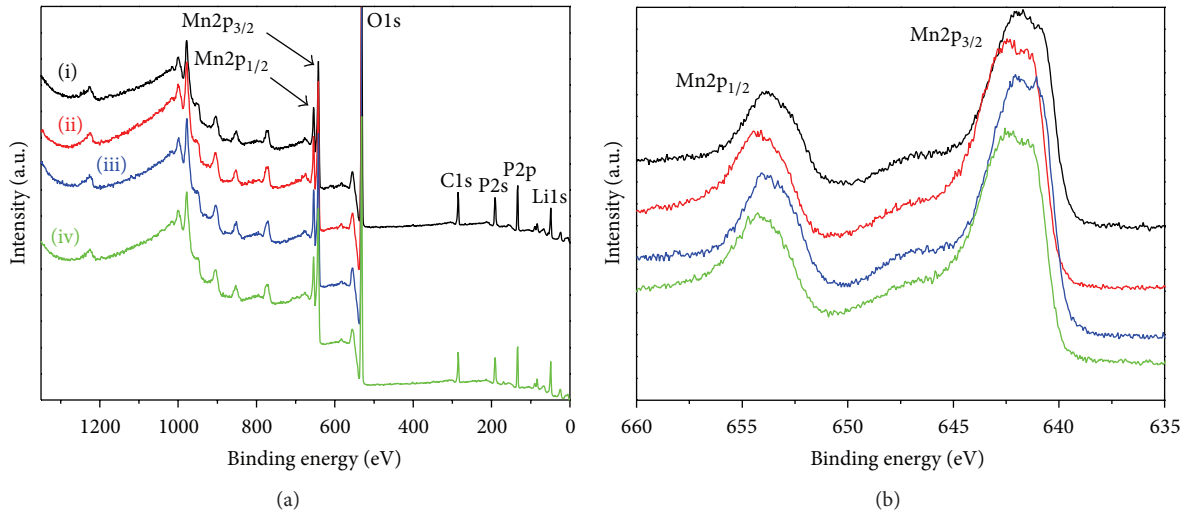

Figure 2: (a) XPS wide scan spectrum and (b) narrow scan Mn2p spectrum for $LiMnPO_4$ using various precursors: (i) sample A, (ii) sample B, (iii) sample C, and (iv) sample D.

Table 3: ICP results of $LiMnPO_4$ using various precursors.

Sample	Li	Mn	P
Sample A	0.80	1.00	0.90
Sample B	0.87	1.00	0.92
Sample C	0.06	1.00	0.76
Sample D	0.14	1.00	0.79

larger amount of Mn^{2+} might exist in samples A and B. Lee et al. [26] previously reported that the binding energy of $Mn2p_{3/2}$ for Mn^{2+} and Mn^{3+} is 641.1 eV and 642.3 eV, which is consistent with the present data.

In order to further investigate the gap between atomic ratio of Li : Mn : P for as-prepared $LiMnPO_4$ and stoichiometric ratio, inductively coupled plasma (ICP-OES) was carried out. As shown in Table 3, samples synthesized from $MnSO_4$ (samples C and D) contain very small amount of Li. However, samples synthesized from MnAc (samples A and B) contain large amount of Li. This Li deficiency is corresponding to Li vacancy which is termed on Li defects in this paper. It is also found that sample B contains smaller Li deficiency than that of sample A. The difference in the Li deficiency is probably due to the difference in basic strength of LiOH (strong basic) and LiAc (weak basic). It was previously reported that hydrothermal reaction using basic solution is suitable for the synthesis of $LiMnPO_4$ [15]. In addition, as the amount of Li increases, the amount of P also increases.

As shown in Figures 3(a)–3(d) prismatic shape is observed at all as-prepared $LiMnPO_4$ samples, and particle sizes of samples C and D are around 10~20 μm, while samples A and B are in micrometer order.

Cycling performance and galvanostatic charge and discharge curves at 1st, 10th, 30th, and 50th cycle are shown in Figures 4(a)–4(e). Galvanostatic charge and discharge

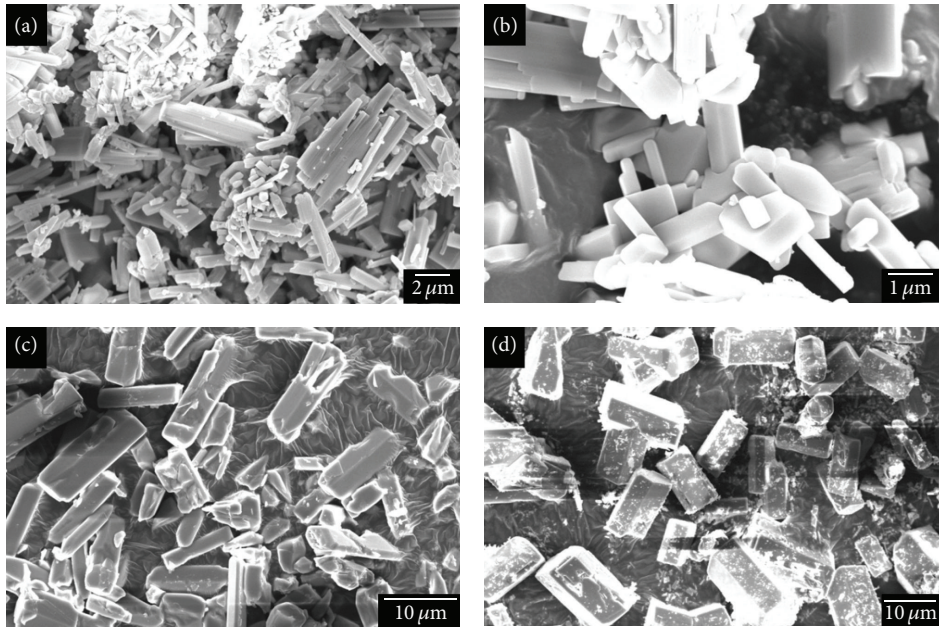

Figure 3: SEM images of $LiMnPO_4$ using various precursors: (a) sample A, (b) sample B, (c) sample C, and (d) sample D.

curves of samples synthesized from MnAc (samples A and B) indicate coexistence of plateau of $LiMnPO_4$ and $MnPO_4$ near 4 V with 40 mAh/g discharge capacity at 1/20 *C* rate. However, no obvious redox plateau is observed from samples synthesized from $MnSO_4$ (samples C and D) whose capacity is less than 10 mAh/g. These results are consistent with XRD results and Li content information obtained from ICP data that the sample prepared from MnAC and LiOH contains higher quality olivine structure and less impurity. Besides, discharge capacity increases as a function of cycle number for all samples. The discharge capacity of sample A and sample B reached 40.6 mAh/g at the 50th cycle from 26.7 mAh/g of the 1st cycle and 45.9 mAh/g at the 50th cycle from 12.8 mAh/g of the 1st cycle, respectively. Referring to ICP data, this phenomenon may be due to the gradual insertion of Li ion into the Li defect as the cycle number increases.

3.2. Various Parameters for Hydrothermal Synthesis. Since $LiMnPO_4$ using LiOH and MnAc shows larger discharge capacity, therefore hydrothermal parameters including temperature and $[H_2O]/[Mn]$ value were further investigated by using LiOH, MnAc, and $NH_4H_2PO_4$ as precursors. The hydrothermal temperature was set from 150°C to 190°C for 12 hours, and $[H_2O]/[Mn]$ value was set as 15 or 30 (Table 4). After hydrothermal, reaction as-prepared powder was rinsed by distilled water and ethanol as the same as the above.

The XRD patterns for all $LiMnPO_4$ samples shown in Figure 5 indicate olivine structure derived from $LiMnPO_4$ without any impurity. No significant difference was detected among the sample prepared between various conditions.

The XPS spectra and binding energy of Mn2p shown in Figures 6(a) and 6(b) display similar spectra and binding energy of $Mn2p_{3/2}$ around 641.6 eV. Therefore, Mn oxidation state is mainly influenced by Mn source rather than the hydrothermal condition, temperature, and $[H_2O]/[Mn]$ value.

Table 4: Binding energy of $Mn2p_{3/2}$ for $LiMnPO_4$ synthesized with various parameters.

Sample	$Mn2p_{3/2}$ [eV]
Sample B 190°C $[H_2O]/[Mn] = 30$	641.57
Sample E 190°C $[H_2O]/[Mn] = 15$	641.67
Sample F 150°C $[H_2O]/[Mn] = 30$	641.73
Sample G 150°C $[H_2O]/[Mn] = 15$	641.55

Table 5: ICP results of $LiMnPO_4$ synthesized with various parameters.

Sample	Li	Mn	P
Sample B 190°C $[H_2O]/[Mn] = 30$	0.87	1.00	0.92
Sample E 190°C $[H_2O]/[Mn] = 15$	0.89	1.00	0.91
Sample F 150°C $[H_2O]/[Mn] = 30$	0.84	1.00	0.88
Sample G 150°C $[H_2O]/[Mn] = 15$	0.88	1.00	0.92

ICP results listed in Table 5 indicate that Li and P defects are observed in all $LiMnPO_4$ samples and the amounts of Li and P defects are about 13% and 9%, respectively. It is easy to

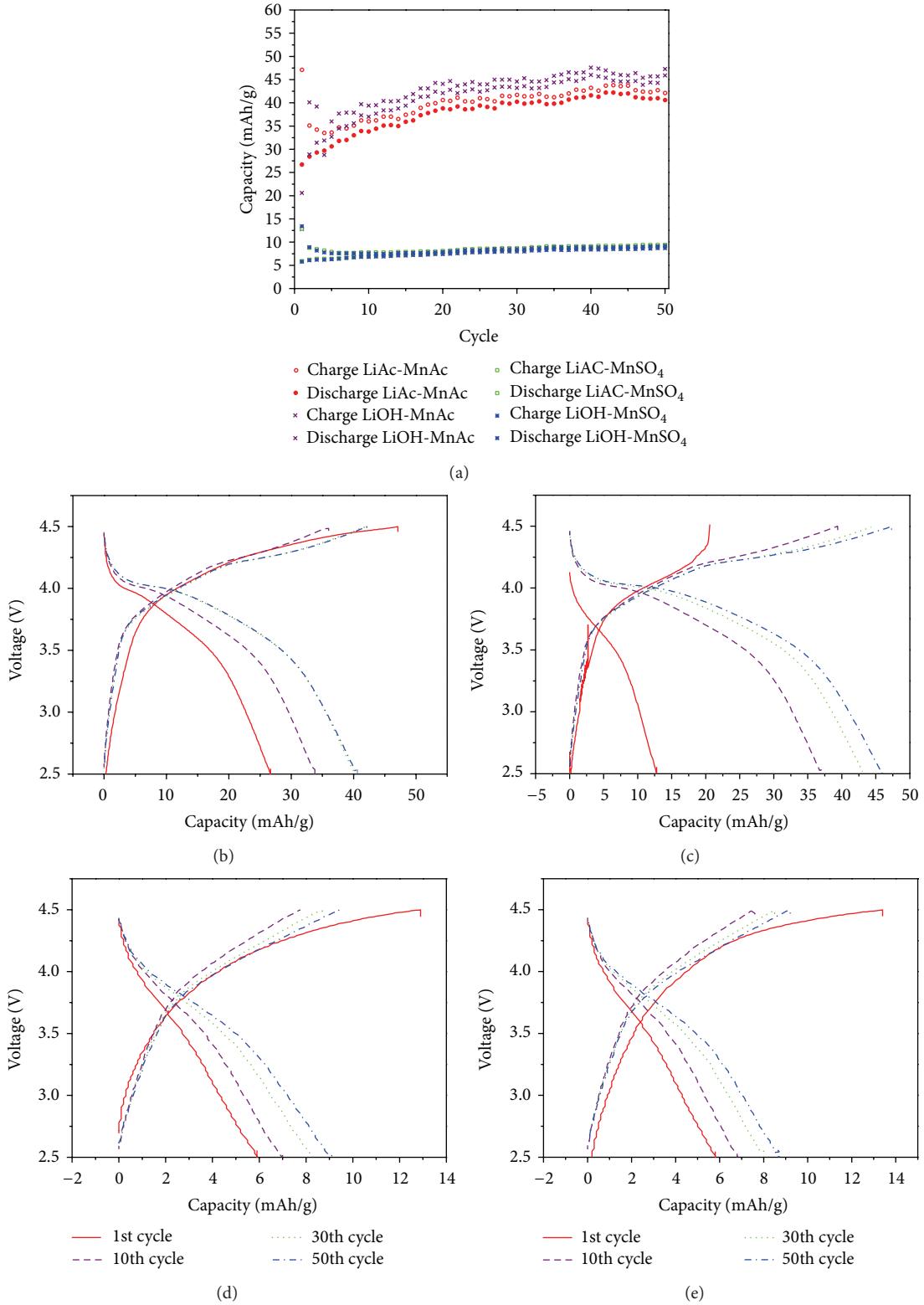

Figure 4: (a) Cycle property of $LiMnPO_4$ using various precursors and charge-discharge curve: (b) sample A, (c) sample B, (d) sample C, and (e) sample D.

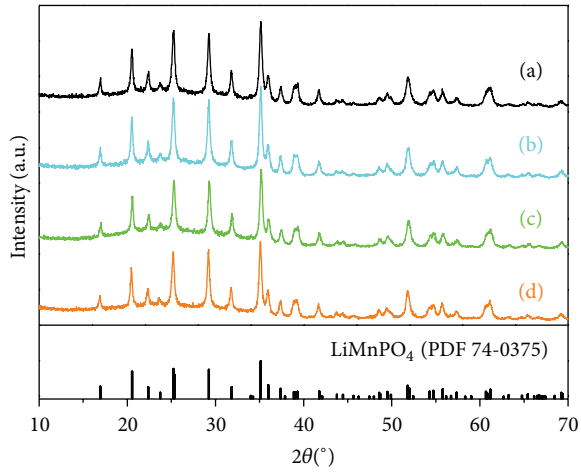

FIGURE 5: XRD pattern for $LiMnPO_4$ synthesized with various parameters: (a) 190°C $[H_2O]/[Mn] = 30$ (sample B), (b) 190°C $[H_2O]/[Mn] = 15$ (sample E), (c) 150°C $[H_2O]/[Mn] = 30$ (sample F), and (d) 150°C $[H_2O]/[Mn] = 15$ (sample G).

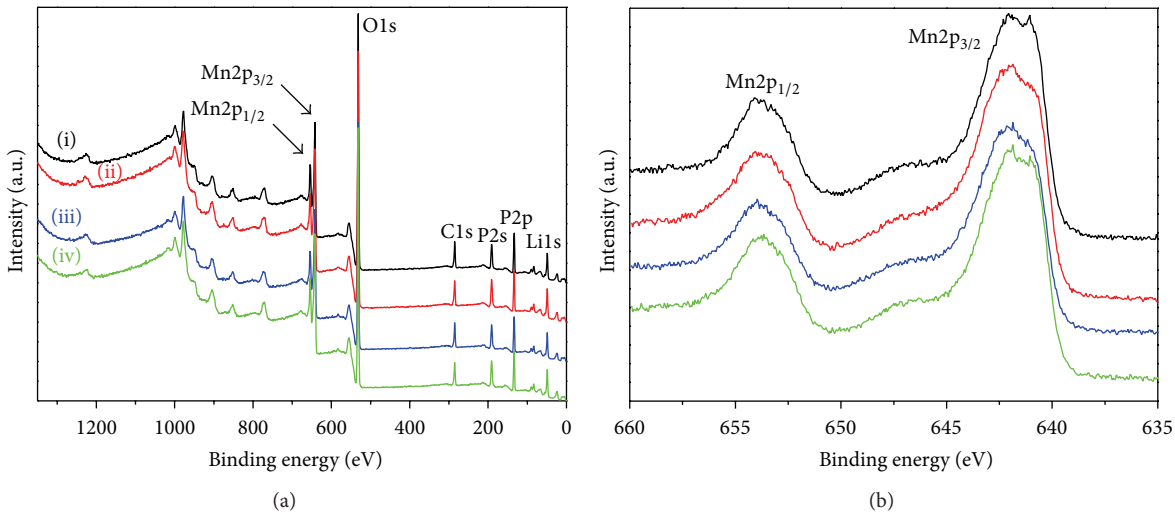

FIGURE 6: (a) XPS wide scan spectrum, (b) narrow scan Mn2p spectrum for $LiMnPO_4$ synthesized with various parameters: (i) 190°C $[H_2O]/[Mn] = 30$ (sample B), (ii) 190°C $[H_2O]/[Mn] = 15$ (sample E), (iii) 150°C $[H_2O]/[Mn] = 30$ (sample F), and (iv) 150°C $[H_2O]/[Mn] = 15$ (sample G).

lose Li and P during the hydrothermal reaction. Therefore, it is suggested that excess Li and P are used as precursors, which is consistent with the previously reported results [10, 14–19].

Since no impurity is detected by XRD, Raman spectroscopy is used to detect excess Li, Mn, and P compounds which might exist in $LiMnPO_4$ as impurity. It is previously reported [13, 27] that $LiMnPO_4$ sample contained $Mn_2P_2O_7$ and Li_3PO_4 as impurity. However, no such impurity is detected in our sample. Figure 7 shows that the Raman spectra of as-prepared $LiMnPO_4$ are consistent with the previously reported data [28]. The Raman data suggests that the as-prepared sample only contains single phase $LiMnPO_4$ without impurities such as $Mn_2P_2O_7$ or Li_3PO_4.

The SEM images of each $LiMnPO_4$ particle are presented in Figures 8(a)–8(d). As-prepared $LiMnPO_4$ powder of sample B shows a particle size over 1 μm. Grain growth was restricted as reducing hydrothermal temperature and $[H_2O]/[Mn]$ value. Sample G has the smallest particle size among them. Moreover, particle morphology changes from prismatic shape to thin plate shape.

The electrochemical performances were summarized in Figures 9(a)–9(e). Sample G shows the largest discharge capacities, which was as high as 39.0 mAh/g at the 1st cycle and 68.7 mAh/g at the 50th cycle. Other samples do not show large discharge capacities. However, each sample shows different discharge capacities in the 1st cycle. In addition, discharge capacity in each cycle becomes large as a function of cycle number. The presence of Li defect in the samples might be responsible for increasing discharge capacity.

4. Conclusions

High purity $LiMnPO_4$ was synthesized by hydrothermal method with different precursors and conditions. Different

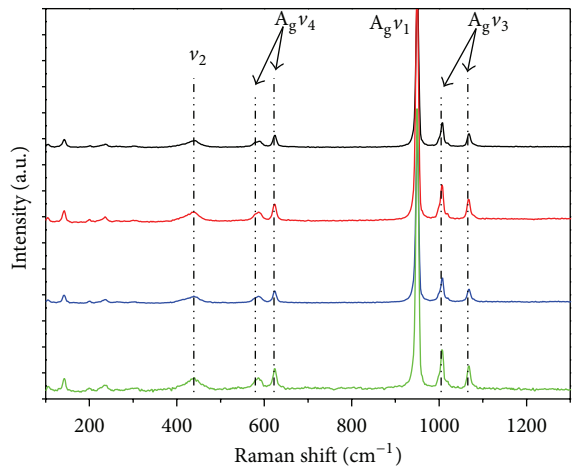

FIGURE 7: Raman spectrum for $LiMnPO_4$ synthesized with various parameters: (a) 190°C $[H_2O]/[Mn]$ = 30 (sample B), (b) 190°C $[H_2O]/[Mn]$ = 15 (sample E), (c) 150°C $[H_2O]/[Mn]$ = 30 (sample F), and (d) 150°C $[H_2O]/[Mn]$ = 15 (sample G).

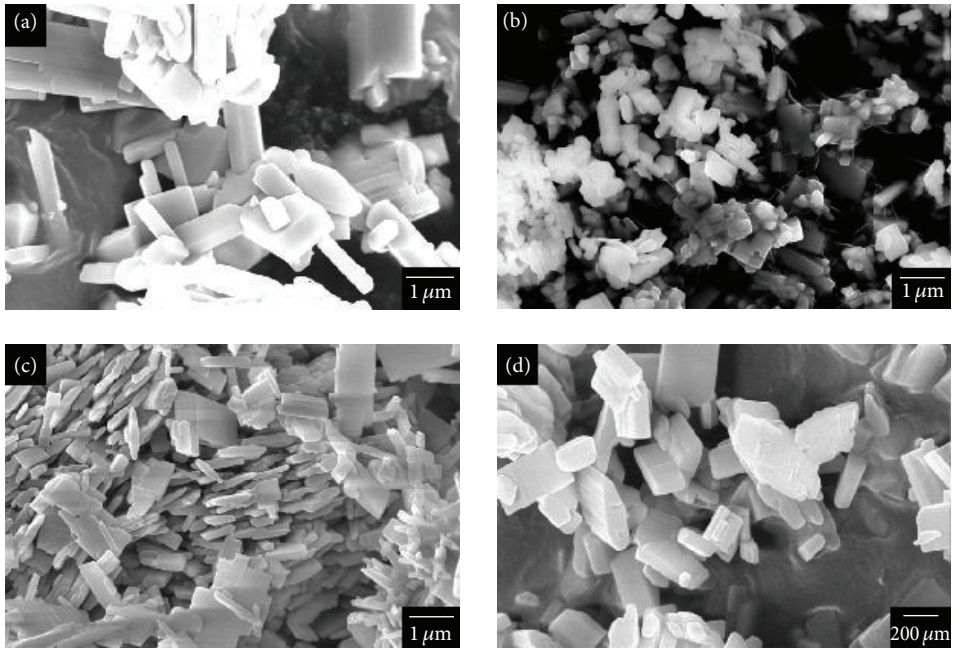

FIGURE 8: SEM images of $LiMnPO_4$ synthesized with various parameters: (a) 190°C $[H_2O]/[Mn]$ = 30 (sample B), (b) 190°C $[H_2O]/[Mn]$ = 15 (sample E), (c) 150°C $[H_2O]/[Mn]$ = 30 (sample F), and (d) 150°C $[H_2O]/[Mn]$ = 15 (sample G).

synthesis condition results in different characteristics. In case of precursors, samples synthesized from $MnSO_4$ hardly contain lithium and do not have olivine structure, and they do not show charge and discharge reaction between Mn^{2+} and Mn^{3+}. However, samples synthesized from MnAc have olivine structure without impurity and show charge and discharge reaction of Mn^{2+}/Mn^{3+} although these $LiMnPO_4$ synthesized from MnAc contain some Li and P defects. For Li source, the sample synthesized from LiOH shows better discharge capacity than that of LiAc. In the case of hydrothermal condition, as the temperature and the $[H_2O]/[Mn]$ values are decreased, smaller particle size and larger capacity were obtained. The precursor molar ratio of Li : Mn : P was set at 1 : 1 : 1 to synthesize $LiMnPO_4$ by hydrothermal reaction, which results in a slight deficiency of Li and P. Therefore, it is important to adjust Li and P precursor molar ratios for synthesizing stoichiometric $LiMnPO_4$.

Conflict of Interests

The authors declare that there is no conflict of interests regarding the publication of this paper.

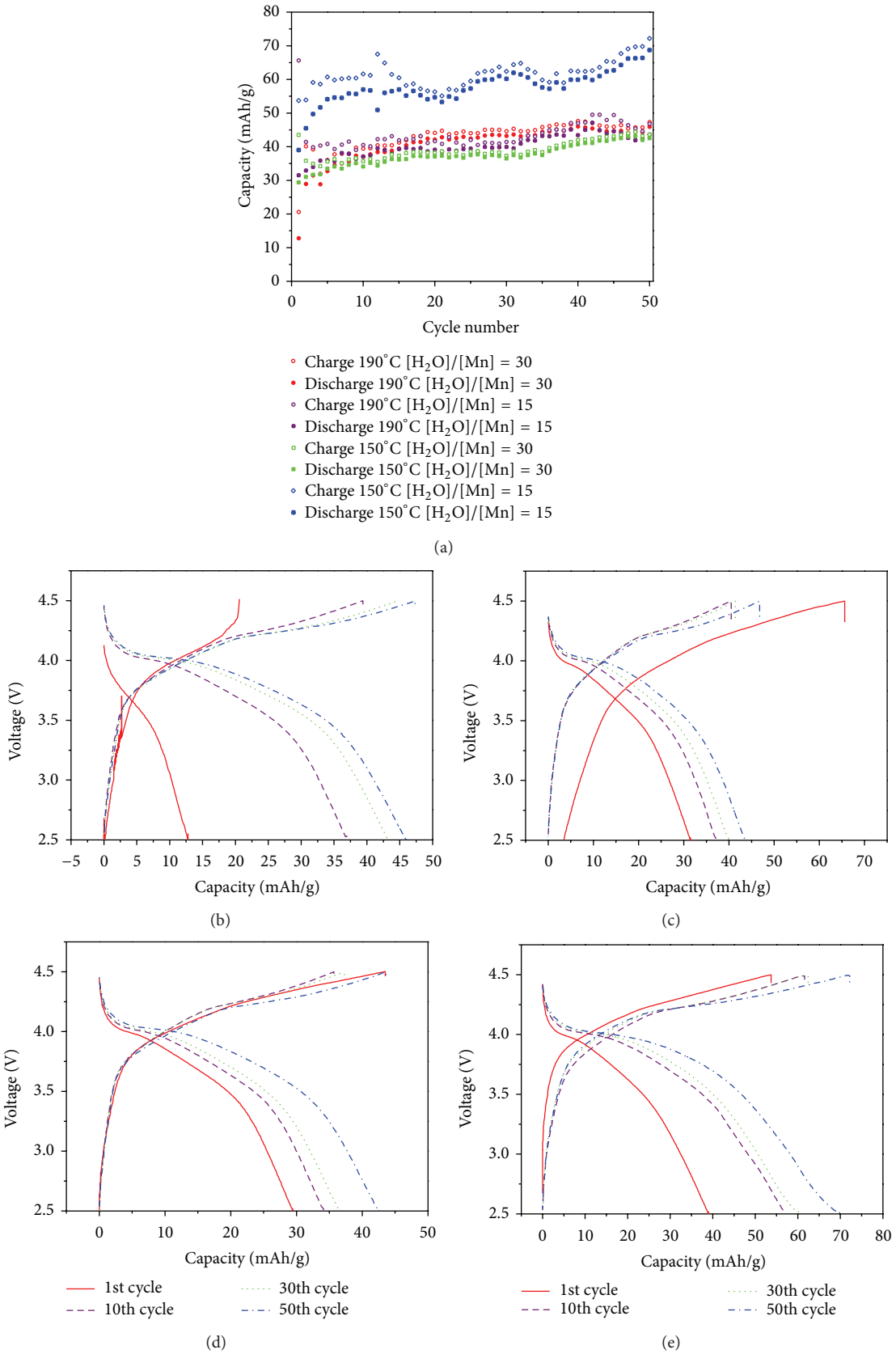

Figure 9: (a) Cycle property of $LiMnPO_4$ synthesized with various parameters: (b) 190°C $[H_2O]/[Mn] = 30$ (sample B), (c) 190°C $[H_2O]/[Mn] = 15$ (sample E), (d) 150°C $[H_2O]/[Mn] = 30$ (sample F), and (e) 150°C $[H_2O]/[Mn] = 15$ (sample G).

Acknowledgments

This research work was carried out under a Joint Education Program between Tsinghua University and Tohoku University. The authors wish to thank Mr. Naoaki Kuwata and Mr. M. T. Chowdhury for the valuable suggestions.

References

[1] K. Mizushima, P. C. Jones, P. J. Wiseman, and J. B. Goodenough, "Li_xCoO_2 ($0 < \mathbf{x} < -1$): a new cathode material for batteries of high energy density," *Materials Research Bulletin*, vol. 15, no. 6, pp. 783–789, 1980.

[2] G. G. Amatucci, J. M. Tarascon, and L. C. Klein, "Cobalt dissolution in $LiCoO_2$-based non-aqueous rechargeable batteries," *Solid State Ionics*, vol. 83, no. 1-2, pp. 167–173, 1996.

[3] A. K. Padhi, K. S. Nanjundaswamy, and J. B. Goodenough, "Phospho-olivines as positive-electrode materials for rechargeable lithium batteries," *Journal of the Electrochemical Society*, vol. 144, no. 4, pp. 1188–1194, 1997.

[4] A. K. Padhi, K. S. Nanjunclaswamy, C. Masquelier, S. Okada, J. B. Gooclenough, and J. Electrochem, "Effect of structure on the Fe^{3+}/Fe^{2+} redox couple in iron phosphates," *Journal of The Electrochemical Society*, vol. 144, no. 5, pp. 1609–1613, 1997.

[5] W. F. Howard and R. M. Spotnitz, "Theoretical evaluation of high-energy lithium metal phosphate cathode materials in Li-ion batteries," *Journal of Power Sources*, vol. 165, no. 2, pp. 887–891, 2007.

[6] C. Delacourt, L. Laffont, R. Bouchet et al., "Toward understanding of electrical limitations (electronic, ionic) in $LiMPO_4$ (M = Fe, Mn) electrode materials," *Journal of the Electrochemical Society*, vol. 152, no. 5, pp. A913–A921, 2005.

[7] J. Kim, K.-Y. Park, I. Park et al., "The effect of particle size on phase stability of the delithiated Li_xMnPO_4," *Journal of the Electrochemical Society*, vol. 159, no. 1, pp. A55–A59, 2012.

[8] D. Choi, D. Wang, I. Bae et al., "$LiMnPO_4$ nanoplate grown via solid-state reaction in molten hydrocarbon for Li-ion battery cathode," *Nano Letters*, vol. 10, no. 8, pp. 2799–2805, 2010.

[9] T. Drezen, N.-H. Kwon, P. Bowen, I. Teerlinck, M. Isono, and I. Exnar, "Effect of particle size on $LiMnPO_4$ cathodes," *Journal of Power Sources*, vol. 174, no. 2, pp. 949–953, 2007.

[10] J. Yoshida, M. Stark, J. Holzbock et al., "Analysis of the size effect of $LiMnPO_4$ particles on the battery properties by using STEM-EELS," *Journal of Power Sources*, vol. 226, pp. 122–126, 2013.

[11] T. Kim, H. Park, M. Lee, S. Lee, and H. Song, "Restricted growth of $LiMnPO_4$ nanoparticles evolved from a precursor seed," *Journal of Power Sources*, vol. 210, pp. 1–6, 2012.

[12] J. Xiao, W. Xu, D. Choi, and J. Zhang, "Synthesis and characterization of lithium manganese phosphate by a precipitation method," *Journal of the Electrochemical Society*, vol. 157, no. 2, pp. A142–A147, 2010.

[13] C. Delacourt, P. Poizot, M. Morcrette, J.-M. Tarascon, and C. Masquelier, "One-step low-temperature route for the preparation of electrochemically active $LiMnPO_4$ powders," *Chemistry of Materials*, vol. 16, no. 1, pp. 93–99, 2004.

[14] M. K. Devaraju and I. Honma, "Hydrothermal and solvothermal process towards development of $LiMPO_4$ (M = Fe, Mn) nanomaterials for lithium-ion batteries," *Advanced Energy Materials*, vol. 2, no. 3, pp. 284–297, 2012.

[15] C. Neef, C. Jähne, H.-P. Meyer, and R. Klingeler, "Morphology and agglomeration control of $LiMnPO_4$ micro- and nanocrystals," *Langmuir*, vol. 29, no. 25, pp. 8054–8060, 2013.

[16] H. Ji, G. Yang, H. Ni, S. Roy, J. Pinto, and X. Jiang, "General synthesis and morphology control of LiMnPO4 nanocrystals via microwave-hydrothermal route," *Electrochimica Acta*, vol. 56, no. 9, pp. 3093–3100, 2011.

[17] K. Dokko, T. Hachida, and M. Watanabe, "$LiMnPO_4$ nanoparticles prepared through the reaction between Li_3PO_4 and molten aqua-complex of $MnSO_4$," *Journal of the Electrochemical Society*, vol. 158, no. 12, pp. A1275–A1281, 2011.

[18] X.-L. Pan, C.-Y. Xu, and L. Zhen, "Synthesis of $LiMnPO_4$ microspheres assembled by plates, wedges and prisms with different crystallographic orientations and their electrochemical performance," *CrystEngComm*, vol. 14, no. 20, pp. 6412–6418, 2012.

[19] Z. Gao, X. Pan, H. Li, S. Xie, R. Yi, and W. Jin, "Hydrothermal synthesis and electrochemical properties of dispersed $LiMnPO_4$ wedges," *CrystEngComm*, vol. 15, no. 38, pp. 7808–7814, 2013.

[20] F. Zhou, P. Zhu, X. Fu, R. Chen, R. Sun, and C. Wong, "Comparative study of $LiMnPO_4$ cathode materials synthesized by solvothermal methods using different manganese salts," *CrystEngComm*, vol. 16, no. 5, pp. 766–774, 2014.

[21] Z. Qin, X. Zhou, Y. Xia, C. Tang, and Z. Liu, "Morphology controlled synthesis and modification of high-performance $LiMnPO_4$ cathode materials for Li-ion batteries," *Journal of Materials Chemistry*, vol. 22, no. 39, pp. 21144–21153, 2012.

[22] J. Su, B. Wei, J. Rong et al., "A general solution-chemistry route to the synthesis $LiMPO_4$ (M = Mn, Fe, and Co) nanocrystals with [010] orientation for lithium ion batteries," *Journal of Solid State Chemistry*, vol. 184, no. 11, pp. 2909–2919, 2011.

[23] T. N. L. Doan and I. Taniguchi, "Cathode performance of $LiMnPO_4$/C nanocomposites prepared by a combination of spray pyrolysis and wet ball-milling followed by heat treatment," *Journal of Power Sources*, vol. 196, no. 3, pp. 1399–1408, 2011.

[24] S. K. Martha, B. Markovsky, J. Grinblat et al., "$LiMnPO_4$ as an advanced cathode material for rechargeable lithium batteries," *Journal of the Electrochemical Society*, vol. 156, no. 7, pp. A541–A552, 2009.

[25] S. Moon, P. Muralidharan, and D. K. Kim, "Carbon coating by high-energy milling and electrochemical properties of $LiMnPO_4$ obtained in polyol process," *Ceramics International*, vol. 38, no. 1, pp. S471–S475, 2012.

[26] J. Lee, M. Park, B. Anass, J. Park, M. Paik, and S. Doo, "Electrochemical lithiation and delithiation of $LiMnPO_4$: effect of cation substitution," *Electrochimica Acta*, vol. 55, no. 13, pp. 4162–4169, 2010.

[27] P. R. Kumar, M. Venkateswarlu, M. Misra, A. K. Mohanty, and N. Satyanarayana, "Carbon coated $LiMnPO_4$ nanorods for lithium batteries," *Journal of the Electrochemical Society*, vol. 158, no. 3, pp. A227–A230, 2011.

[28] K. P. Korona, J. Papierska, M. Kamińska, A. Witowski, M. Michalska, and L. Lipińska, "Raman measurements of temperature dependencies of phonons in $LiMnPO_4$," *Materials Chemistry and Physics*, vol. 127, no. 1-2, pp. 391–396, 2011.